Optimal Motion Planning for Mobile Welding Robot

Gen Pan[1,2], Enguang Guan[2], Fan Yang[3(✉)], Anye Ren[1], and Peng Gao[1]

[1] Institute of Aerospace System Engineering Shanghai, Shanghai, People's Republic of China
[2] State Key Lab of Mechanical System and Vibration, Shanghai Jiao Tong University, Shanghai, People's Republic of China
[3] Shanghai Aerospace Control Technology Institute, Shanghai, People's Republic of China
Yangfan880109@163.com

Abstract. This paper focuses on the motion planning method for a novel mobile welding robot (MWR), based on the screw theory. The robot consists of a vehicle unit and a 5-DOF manipulator, which equipped a torch at the end of manipulator. In order to finish the welding task, the kinematic motion planning strategy is of great importance. As the traditional strategy which uses inverse kinematic and polynomial interpolation may cause a waste of computing time, the screw theory is chosen to improve the strategy. From the simulation and experiment results, it can be found that the optimal motion planning method is reliable and efficient.

Keywords: Mobile welding robot · Motion planning strategy · Screw theory

1 Introduction

Welding tasks involved in large unstructured equipment building such as ships and oil tankers are challenging and urge to be solved. As the working conditions are space constricted and dangerous, a novel mobile welding robot which can move on the slope or even vertical surfaces of huge equipments can be one potential solution. Recently, several research works have proved that automatic welding technology can improve the quality of welding seams signally [1–3]. Path planning of wheeled welding robots [4–6] and the algorithm research for trajectory planning [7–9] are also helpful for increasing the reliability and the efficiency of the MWR system.

In this paper, the MWR system has a novel combined mechanism for welding tasks. In our research team, Wu [10, 11] has made a detailed introduction about the MWR's structure in the published papers. The vehicle unit consists of three identical mobile adhesion parts and each of them comprises one wheel group, one magnetic adhesion unit and one lifting mechanism. The welding manipulator contains five rotational joints. The welding torch is held at the end of the manipulator.

Using the MWR as the controlled member, an optimal motion planning strategy is proposed. As the traditional strategy which uses inverse kinematic and polynomial

Y. Huang et al. (Eds.): ICIRA 2017, Part II, LNAI 10463, pp. 124–134, 2017.
DOI: 10.1007/978-3-319-65292-4_12

interpolation [12, 13] may cause a waste of computing time, the screw theory model is used to improve the strategy performance. The structure of this paper is as follows: a brief introduction of the MWR is proposed in Sect. 2. The screw model of MWR and the motion planning strategy are presented in Sect. 3. Details about the simulation and experimental evaluation are demonstrated as the result and discussion and presented in Sect. 4. Conclusions are drawn in Sect. 5.

2 Mobile Welding Robot Design

The prototype of MWR is shown in Fig. 1. The MWR consists of one vehicle platform at the bottom and a 5-DOF manipulator arm mounted on the vehicle platform. The welding torch is clamped onto the manipulator. The wheel-foot mechanism of vehicle can move and cross obstacle flexibly adapting to large unstructured equipments, and three permanent-magnetic suction cups can adjust the air gap to control the adsorption force. The MWR has the mobility capability such as walking, climbing wall, crossing obstacles, turning and welding. To achieve a coordinate welding trajectory, need to study the motion planning algorithm insuring computational efficiency and path precision.

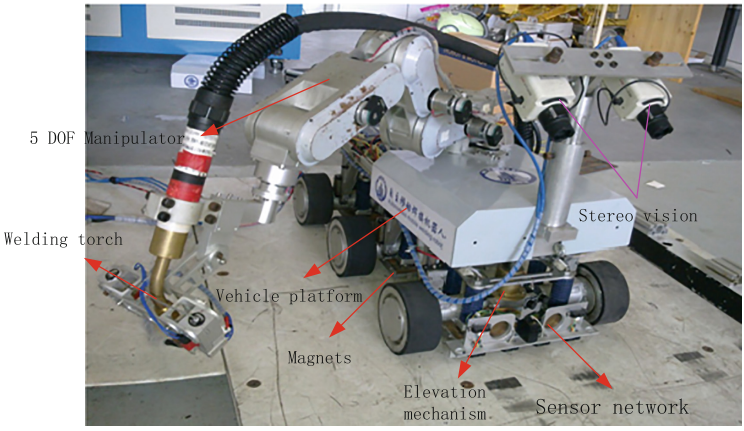

Fig. 1. Prototype of mobile welding robot

The main hardware structure of the control system of WMR is shown in Fig. 2. The control system is composed of an industrial personal computer, servo drivers, servo motors, stereo camera, sensor system, and software. IPC and servo drivers are configured as master-slave construction. Communication link between IPC and drivers or sensor is established by CAN bus. IPC is used for planning and sending mission commands. Servo drivers generate real-time control command of the motors, execute the motion planning and control algorithm, and drive the motors moving.

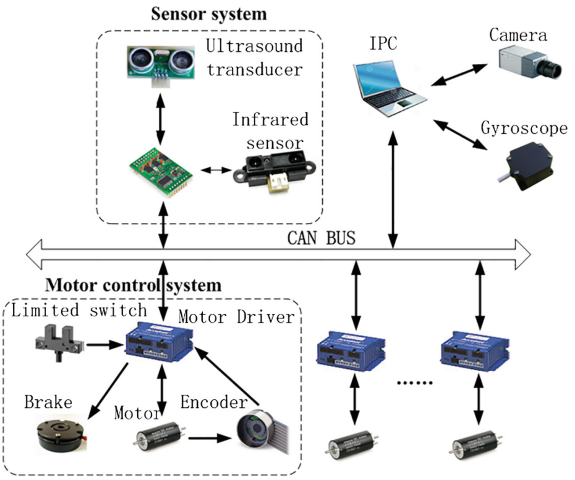

Fig. 2. The structure of hardware system

3 Motion Planning Strategy for MWR

3.1 Kinematical Modeling Based on Screw Theory

Different from the traditional kinematical modeling theory such as D-H theory, screw theory [14] is efficient in rotational and stretching DOF modeling. Under screw theory, the kinematical modeling can be described as follows:

Figure 3 shows the coordinate system of manipulator. If θ_i, $i = 1, 2, \ldots, 5$ do not equals to 0 at the same time, the revolving vectors of the rotation joints can be denoted as:

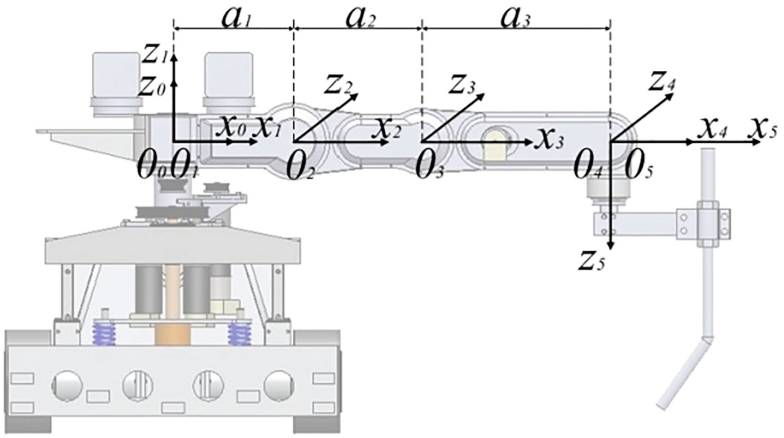

Fig. 3. The coordinate system of manipulator

$$
\begin{aligned}
\$_1 &= (0 \quad 0 \quad 1; 0 \quad 0 \quad 0)\\
\$_2 &= (-s_1 \quad c_1 \quad 0; 0 \quad 0 \quad a_1)\\
\$_3 &= \left(-s_1 \quad c_1 \quad 0; a_2 c_1 s_2 \quad a_2 s_1 s_2 \quad a_1 + a_2 c_2\right)\\
\$_4 &= \left(-s_1 \quad c_1 \quad 0; c_1(a_3 s_{23} + a_2 s_2) \quad s_1(a_3 s_{23} + a_2 s_2) \quad a_1 + a_3 c_{23} + a_2 c_2\right)\\
\$_5 &= (-s_{23} c_1 \quad -s_{23} s_1 \quad -c_{23}; -s_1(a_1 c_{23} + a_2 c_3) \quad c_1(a_1 c_{23} + a_2 c_3) \quad 0)\\
\$_{wl} &= (0 \quad 0 \quad 0; 0 \quad 1 \quad 0)
\end{aligned}
$$

where $\theta_i (i = 1, 2, \ldots, 5)$ is the angle of the *i-th* joint, while $\$_i, i = 1, 2, \cdots, 5$ is the screw vector of the *i-th* rotation joint, and $\$_{wl}$ is the screw vector of the vehicle unit. c_i represents $\cos\theta_i$, and s_i represents $\sin\theta_i$, while c_{ij} and s_{ij} mean $\cos(\theta_i + \theta_j)$ and $\sin(\theta_i + \theta_j)$.

If the linear velocity of the vehicle unit is v_{wl}, and the rotational velocity of each rotation joint is $\omega_i,\ i = 1,\ 2,\ \cdots,\ 5$, the screw vector at the end of the manipulator can be denoted as:

$$
\$_m = v_{wl}\$_{wl} + \sum_{i=1}^{5} \omega_i \$_i = \begin{bmatrix} -s_1(\omega_2 + \omega_3 + \omega_4 + \omega_5) \\ c_1(\omega_2 + \omega_3 + \omega_4 + \omega_5) \\ \omega_1 \\ a_2 c_1 s_2 \omega_3 + c_1(a_3 s_{23} + a_2 s_2)(\omega_4 + \omega_5) \\ v_{wl} + a_2 s_1 s_2 \omega_3 + s_1(a_3 s_{23} + a_2 s_2)(\omega_4 + \omega_5) \\ a_1\omega_2 + (a_1 + a_2 c_2)\omega_3 + (a_1 + a_3 c_{23} + a_2 c_2)(\omega_4 + \omega_5) \end{bmatrix} \quad (1) \qquad (1)
$$

For each joint, the motion ability is limited. That means $v_{wl\_\max} \le v_{wl} \le v_{wl\_\min}$ and $\omega_{i\_\max} \le \omega_i \le \omega_{i\_\min},\ i = 1,\ 2,\ \cdots,\ 5$.

3.2 Linear Motion Modeling Based on Screw Theory

The linear trajectory which is the most common in the welding task is chosen as the motion target. Based on the screw theory, Eq. (1) can be rewritten as, $\$_m = (\boldsymbol{S}_m; \boldsymbol{S}_m^0)$, $\boldsymbol{S}_m = \$_m(1:3)$, $\boldsymbol{S}_m^0 = \$_m(4:6)$. $\$_m$ is a linear screw only when $\mathbf{S}_m = \mathbf{0}$. Then $\omega_1 = 0$ and $\omega_2 + \omega_3 + \omega_4 + \omega_5 = 0$, we can get:

$$
\$_m = \begin{bmatrix} 0 \\ 0 \\ 0 \\ a_2 c_1 s_2 \omega_3 + c_1(a_3 s_{23} + a_2 s_2)(\omega_4 + \omega_5) \\ v_{wl} + a_2 s_1 s_2 \omega_3 + s_1(a_3 s_{23} + a_2 s_2)(\omega_4 + \omega_5) \\ a_1\omega_2 + (a_1 + a_2 c_2)\omega_3 + (a_1 + a_3 c_{23} + a_2 c_2)(\omega_4 + \omega_5) \end{bmatrix}
$$

As the target trajectory is linear, the direction can be denoted as $\mathbf{S}_m^0/\left\|\mathbf{S}_m^0\right\|$ and the velocity is $\left\|\mathbf{S}_m^0\right\|$, where $\|\bullet\|$ is the screw vector modulus. Then we can get:

$$\$_m^0 = \begin{bmatrix} a_2c_1s_2\omega_3 + c_1(a_3s_{23} + a_2s_2)(\omega_4 + \omega_5) \\ v_{wl} + a_2s_1s_2\omega_3 + s_1(a_3s_{23} + a_2s_2)(\omega_4 + \omega_5) \\ a_1\omega_2 + (a_1 + a_2c_2)\omega_3 + (a_1 + a_3c_{23} + a_2c_2)(\omega_4 + \omega_5) \end{bmatrix} \tag{2}$$

In Eq. (2), $\omega_1 = 0$, θ_1 is constant and θ_i, $i = 2, 3, \cdots, 5$ is variable, under $\omega_j \neq 0$, $j = 2, 3, \cdots, 5$. If the target velocity (v_x, v_y, v_z) is known, we can get:

$$\begin{cases} \omega_2 + \omega_3 + \omega_4 + \omega_5 = 0 \\ a_2c_1s_2\omega_3 + c_1(a_3s_{23} + a_2s_2)(\omega_4 + \omega_5) = v_x \\ v_{wl} + a_2s_1s_2\omega_3 + s_1(a_3s_{23} + a_2s_2)(\omega_4 + \omega_5) = v_y \\ a_1\omega_2 + (a_1 + a_2c_2)\omega_3 + (a_1 + a_3c_{23} + a_2c_2)(\omega_4 + \omega_5) = v_z \end{cases} \tag{3}$$

Equation (3) can be simplified by setting $\omega_{45} = \omega_4 + \omega_5$. Then it turns to:

$$\begin{cases} \omega_2 + \omega_3 + \omega_{45} = 0 \\ a_2c_1s_2\omega_3 + c_1(a_3s_{23} + a_2s_2)\omega_{45} = v_x \\ v_{wl}c_1 = v_yc_1 - v_xs_1 \\ a_2c_2\omega_3 + (a_3c_{23} + a_2c_2)\omega_{45} = v_z \end{cases}$$

The solution can be calculated as:

$$\begin{aligned} v_{wl} &= v_y - v_x\tan(\theta_1) \\ \omega_3 &= -\frac{v_xa_3c_{23} + v_xa_2c_2 - v_zc_1(a_3s_{23} + a_2s_2)}{a_2a_3c_1s_3} \\ \omega_{45} &= \frac{v_xc_2 - v_zc_1s_2}{a_3c_1s_3} \\ \omega_2 &= -\omega_3 - \omega_{45} \end{aligned}$$

By the previous velocity constraints, we can get:

$$\begin{cases} v_{wl\_Min} \le v_{wl} \le v_{wl\_Max} \\ \omega_{2\_Min} \le \omega_2 \le \omega_{2\_Max} \\ \omega_{3\_Min} \le \omega_3 \le \omega_{3\_Max} \\ \omega_{4\_Min} + \omega_{5\_Min} \le \omega_{45} \le \omega_{4\_Max} + \omega_{5\_Max} \end{cases}$$

Then

$$\begin{cases} v_{wl\_Min} \le v_y - v_x\tan(\theta_1) \le v_{wl\_Max} \\ \omega_{2\_Min} \le -\omega_3 - \omega_{45} \le \omega_{2\_Max} \\ a_2a_3c_1s_3\omega_{3\_Min} \le -v_x(a_3c_{23} + a_2c_2) + v_zc_1(a_3s_{23} + a_2s_2) \le a_2a_3c_1s_3\omega_{3\_Max} \\ a_3c_1s_3(\omega_{4\_Min} + \omega_{5\_Min}) \le v_xc_2 - v_zc_1s_2 \le a_3c_1s_3(\omega_{4\_Max} + \omega_{5\_Max}) \end{cases}$$

Finally

$$\begin{cases} (a_3c_{23}+a_2c_2)\omega_{45\_Min}+a_2c_2\omega_{3\_Min} \le v_z \le (a_3c_{23}+a_2c_2)\omega_{45\_Max}+a_2c_2\omega_{3\_Max} \\ a_2c_1s_2\omega_{3\_Min}+c_1(a_3s_{23}+a_2s_2)\omega_{45\_Min} \le v_x \le c_1(a_3s_{23}+a_2s_2)\omega_{45\_Max}+a_2c_1s_2\omega_{3\_Max} \\ a_2c_1s_3\omega_{2\_Min} \le v_xc_{23}-v_zc_1s_{23} \le a_2c_1s_3\omega_{2\_Max} \\ v_{wl\_Min} \le v_y - v_x\tan(\theta_1) \le v_{wl\_Max} \end{cases} \tag{4}$$

where $\omega_{45\_Min}=\omega_{4\_Min}+\omega_{5\_Min}$, $\omega_{45\_Max}=\omega_{4\_Max}+\omega_{5\_Max}$.

By using Eq. (4), the proper rotational velocity can be found for each target velocity $(v_x,\ v_y,\ v_z)$.

3.3 Optimal Motion Planning Strategy for MWR

In the traditional motion planning strategy based on D-H inverse kinematics theory, the points containing the position and pose information along the target trajectory are calculated one by one. The density of the points is depended on the accuracy requirement. All of the position and pose information between two points can be calculated by using polynomial interpolation. Therefore if the density of the points is too high, the inverse kinematics calculation will waste extra time; otherwise tracking error will be unacceptable, even may cause the system shock.

Under the previous screw theory model, if each joint angle is known and there is no velocity jump point, the modulated velocity processes will be smoothly and the instantaneous velocity direction at the end of the manipulator will keep along the target trajectory. In this ideal model, the joint angle, rotation velocity and the target velocity at the end of the manipulator can be related by an analytical expression. But in the discrete control mode, the joint angle is nonlinear to the velocity, and there is no analytical solution.

Considering the motion accuracy and instantaneity demands, an optimal motion planning strategy for MWR is designed. In this strategy, if the tracking error is under the threshold value, the screw model is chosen to finish the planning calculation. Otherwise, the D-H inverse kinematics model is chosen to get the tracking error back to the threshold value. The planning process is shown in Fig. 4.

The basic procedures of motion planning algorithm are exAApressed as follows:

(1) Initialize each joint angle and the linear velocity vector of MWR. If the position at the end of the manipulator is out of the work space, the controller will drive the MWR back to the work space.
(2) Initialize the step parameter, including step time, step linear distance and the maximum step joint angle. According to the MWR configuration, θ_2 and θ_3 are sensitive to the linearity of screw vector. Thus after ω_2 and ω_3 are calculated, the bigger one is chosen as the maximum step joint angle.
(3) According to the step parameters, calculate the joint angle, rotation velocity. Then drive the MWR motion.

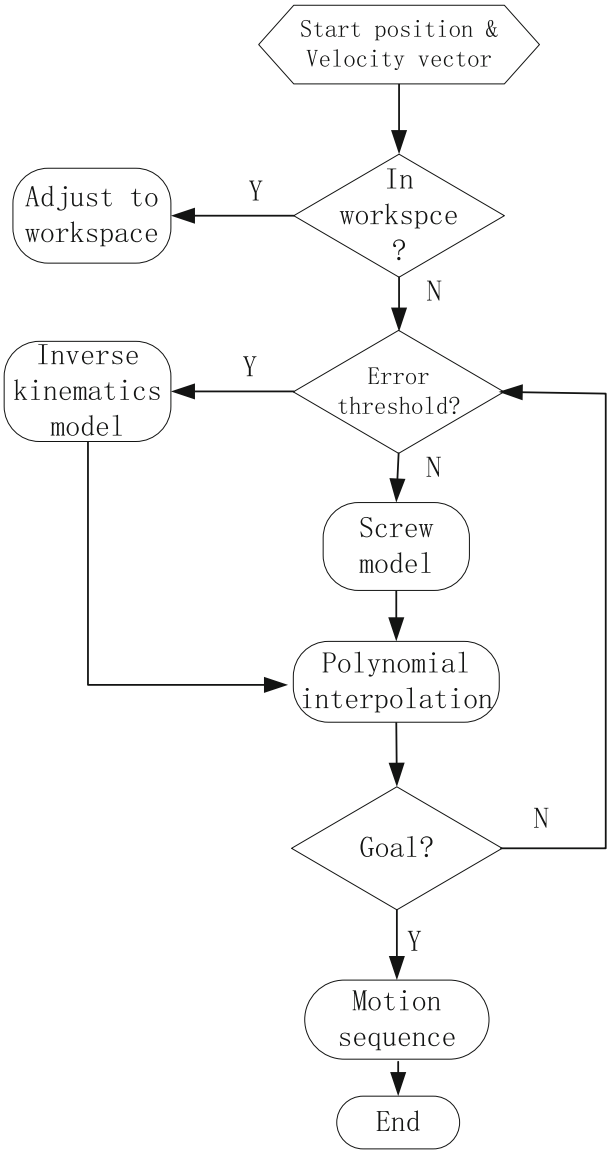

Fig. 4. The flow diagram of the motion planning strategy

(4) During the step motion, the rotation velocity constraints can forbid the velocity jump. Considering the beginning velocity, ending velocity and the motion accuracy demand, polynomial interpolation is used to calculate the joint angle and the rotation velocity.
(5) If the tracking error is under the threshold value, the screw model is chosen to calculate the step parameters. Otherwise, the D-H inverse kinematics model is chosen to get the tracking error back to the threshold value.

4 Simulation and Experiment

The linear trajectory motion planning of MWR was simulated on MATLAB, running on a desktop with a CPU Pentium E5200 Dual-Core, RAM 4 GB. The joint angle vector was initialized as $(0,\ -\pi/3,\ \pi/3,\ 0,\ 0)$; the target velocity was initialized as $(1,\ 0,\ 0)$, the velocity unit was mm/s; the simulation time duration was 50 s; the length of the linear trajectory is 50 mm. In the working space, the fixed X-Y-Z angle coordinate system is chosen to describe the terminal position of the manipulator. The angle coordinate values can be calculated by:

$$\beta = A\tan 2(-r_{31},\ \sqrt{r_{11}^2 + r_{21}^2})$$
$$\alpha = A\tan 2(r_{21}/c\beta,\ r_{11}/c\beta)$$
$$\gamma = A\tan 2(r_{32}/c\beta,\ r_{33}/c\beta)$$

Where r_{ij} is the homogeneous transform matrix element of the tool frame, and $c\beta$ means $\cos\beta$.

In order to evaluate the modified motion planning strategy, the strategies only containing D-H inverse kinematics theory and screw theory are taken into the simulations at the same time.

The simulation results in Fig. 5 indicate that the linear motion process under D-H inverse kinematics theory is smooth and the tracking error is acceptable. The whole simulation time which does not contain the inverse operation of Jacobian matrix and polynomial interpolation is 4.8723 s.

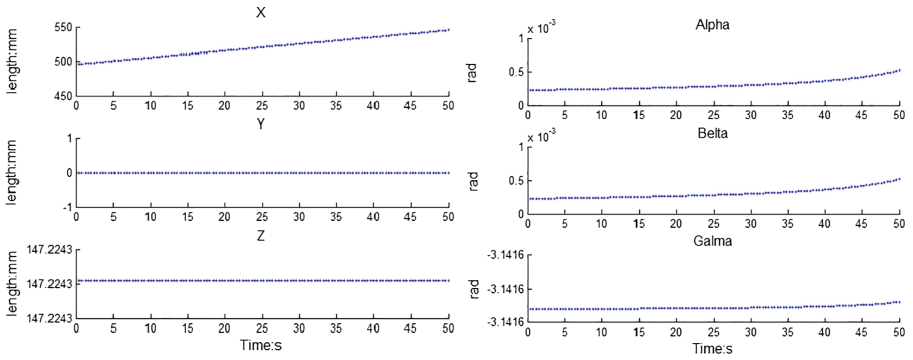

(1) The changes of position (2) The changes of pose

Fig. 5. The simulation results under D-H inverse kinematics theory

The simulation results in Fig. 6 indicate that the linearity of motion under screw theory is worse than the inverse kinematics theory, especially in Z-axis. And the tracking error of posture becomes larger with the simulation time. But the whole simulation time is only 1.4029 s.

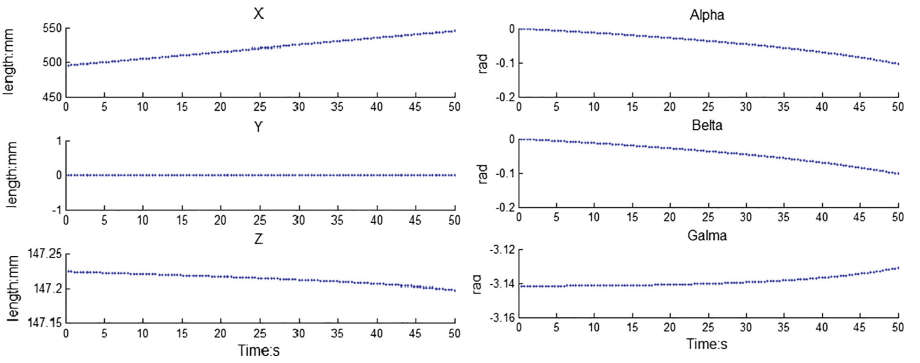

(1) The changes of position (2) The changes of pose

Fig. 6. The simulation results under screw theory

The simulation results under the modified planning strategy are shown in Fig. 7. The threshold value of tracking error is initialized as 0.005 mm. If the tracking error is over the threshold value, the D-H inverse kinematics theory is activated. Thus the changes of position and pose are not continuous. It can be found that the amplitude of the change is limited, such as the amplitude of position change is under 0.0005 mm and the amplitude of pose change is under 0.01. These will not cause the system shock. The whole simulation time is 1.6356 s. It is a little worse than the screw theory, but is more efficient than the inverse kinematics theory. Therefore the optimal motion planning strategy is with a high accuracy and efficient.

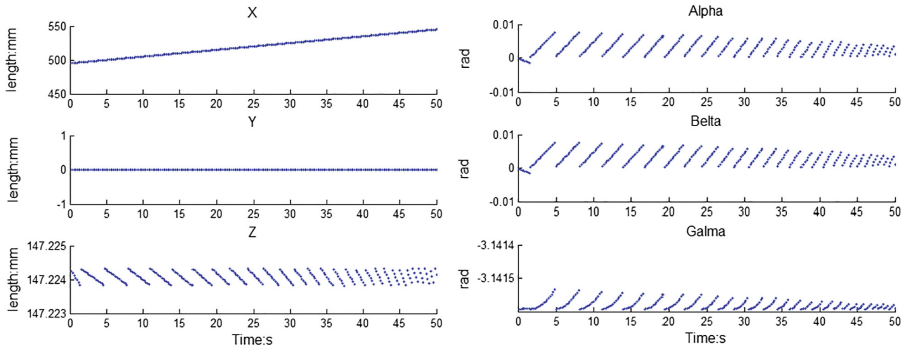

(1) The changes of position (2) The changes of pose

Fig. 7. The simulation results under modified planning strategy

Through the optimization analysis of motion planning algorithm, the modified strategy is verified in the welding experiment. Figure 8(1) shows the welding process. The manipulator adjusts the position and posture to the ready state and then start

welding. When finish welding, remove the torch from the workbench. Figure 8(2) shows the welding effect of the motion planning. The weld length is 50 mm, and result is uniform. It proves that the strategy is effective.

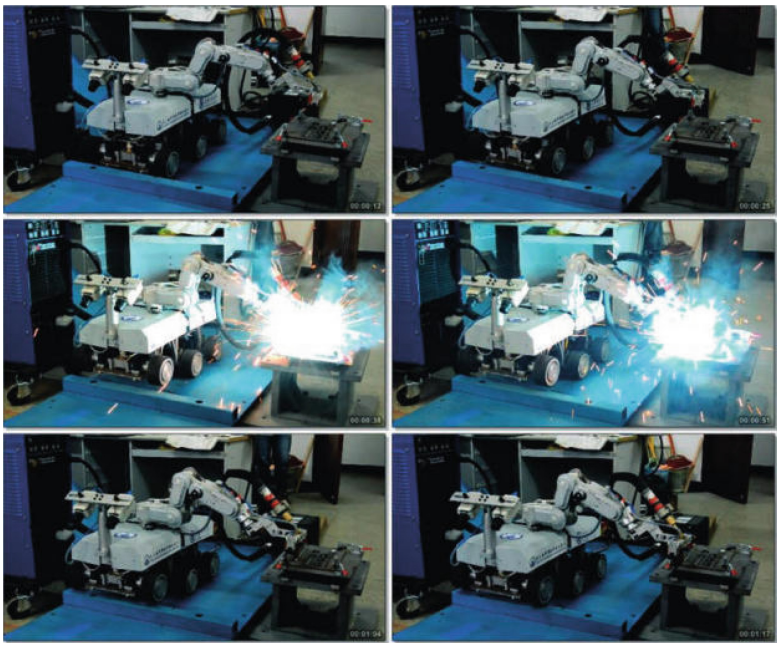

(1) The welding process

(2) The line welding effect

Fig. 8. The welding experiment of MWR

5 Conclusions

This paper has introduced a novel motion planning strategy for MWR. The mechanical structure and control system have been presented. To finish the linear welding task, the kinematic modeling and the motion modeling have been described in detail based on screw theory. Under the optimal motion planning strategy, the MWR is adaptive to the kinds of tracking error. Results from the simulation and experiments have demonstrated

that the motion planning strategy is efficient, and it can be applied confidently in the domain of mobile welding robot systems. The the precision and the reliability will be increased with more sensors in the future.

Acknowledgement. This work is supported by Shanghai Science and Technology Commission Foundation under Grant No. 13DZ1108300, and National 863 plan of China under Grant No. 2009AAA042221.

References

1. Lee, D., Lee, S., Ku, N., Lim, C., Lee, K.Y., Kim, T.W., et al.: Development of a mobile robotic system for working in the double-hulled structure of a ship. Robot. Comput.-Integr. Manuf. **26**(1), 13–23 (2010)
2. Shang, J., Bridge, B., Sattar, T.P., Mondal, S., Brenner, A.: Development of a climbing robot for inspection of long weld lines. Ind. Robot **35**(3), 217–223 (2008)
3. Lee, D., Ku, N., Kim, T.W., Kim, J., Lee, K.Y., Son, Y.S.: Development and application of an intelligent welding robot system for shipbuilding. Robot. Comput.-Integr. Manuf. **27**(2), 377–388 (2011)
4. Nagarajan, U., Kantor, G., Hollis, R.L., (eds.): Trajectory planning and control of an underactuated dynamically stable single spherical wheeled mobile robot. In: IEEE International Conference on Robotics and Automation (2009)
5. Gueta, L.B., Chiba, R., Arai, T., Ueyama, T., Ota, J.: Practical point-to-point multiple-goal task realization in a robot arm with a rotating table. Adv. Robot. **25**(6–7), 717–738 (2011)
6. Toit, N.E.D., Burdick, J.W.: Robot motion planning in dynamic, uncertain environments. IEEE Trans. Robot. **28**(1), 101–115 (2012)
7. Chakraborty, N., Akella, S., Wen, J.T.: Coverage of a planar point set with multiple robots subject to geometric constraints. IEEE Trans. Autom. Sci. Eng. **7**(1), 111–122 (2010)
8. Ngo, M.D., Phuong, N.T., Duy, V.H., Kim, H.K.: Control of two wheeled welding mobile manipulator. Int. J. Adv. Robot. Syst. **4**(3) (2008)
9. Kim, J., Kim, S.R., Kim, S.J., Kim, D.H.: A practical approach for minimum-time trajectory planning for industrial robots. Ind. Robot **37**(1), 51–61 (2010)
10. Wu, M., Gao, X., Yan, W.X., Fu, Z., Zhao, Y., Chen, S.: New mechanism to pass obstacles for magnetic climbing robots with high payload, using only one motor for force-changing and wheel-lifting. Ind. Robot **38**(4), 372–380 (2011)
11. Wu, M., Pan, G., Zhang, T., Chen, S., Zhuang, F., Zhao, Y.Z.: Design and optimal research of a non-contact adjustable magnetic adhesion mechanism for a wall-climbing welding robot. Int. J. Adv. Robot. Syst. **10**(1), 1 (2013)
12. Zhang, T., Chen, S.B.: Optimal posture searching algorithm on mobile welding robot. J. Shanghai Jiaotong Univ. (Sci.) **19**(1), 84–87 (2014)
13. Zhang, T., Wu, M., Zhao, Y., Chen, X., Chen, S.: Optimal motion planning of mobile welding robot based on multivariable broken line seams. Int. J. Robot. Autom. **29**(2), 215–223 (2014)
14. Rodriguez-Leal, E., Dai, J.S., Pennock, G.R.: A study of the kinematics of the 5-RSP parallel mechanism using screw theory. In: Dai, J., Zoppi, M., Kong, X. (eds.) Advances in Reconfigurable Mechanisms and Robots I, pp. 355–369. Springer, London (2012). doi:10.1007/978-1-4471-4141-9_32